Journal of Alloys and Compounds 408–412 (2006) 568–572

Journal of ALLOYS AND COMPOUNDS

www.elsevier.com/locate/jallcom

Additional effects of rare earth elements on formation and properties of some transition metal pyrophosphates

Hiroaki Onoda[a,*], Kazuo Kojima[a], Hiroyuki Nariai[b]

[a] *Department of Materials Science and Engineering, Faculty of Engineering, Kyoto University,*
Yoshida-Honmachi, Sakyo-ku, Kyoto 606-8501, Japan
[b] *Department of Molecular Science and Materials Engineering, Graduate School of Science and Technology,*
Kobe University, 1-1, Rokkodai-cho, Nada-ku, Kobe 657-8501, Japan

Received 30 July 2004; received in revised form 12 October 2004; accepted 15 December 2004

Abstract

Transition metal phosphates have been used as inorganic pigments. By the addition of rare earth elements, new functional materials are expected to form. In this work, rare earth oxides (Y_2O_3, La_2O_3, CeO_2, and Nd_2O_3) were added in the formation systems of copper, manganese, and cobalt pyrophosphates prepared from ammonium dihydrogenphosphate and the transition metal carbonate. The thermal behaviors of the mixtures of ammonium dihydrogenphosphate, transition metal carbonate, and rare earth oxide were investigated with differential thermal analyses, X-ray diffraction, and Fourier transform infrared spectroscopy. Then, thermal products were estimated by particle size distribution, scanning electron micrographs, specific surface area, ultraviolet–visible reflectance spectra, fluorescence spectra, and acid and base resistance. The influence by the addition of rare earth elements was discussed on the kinds of rare earth elements, transition metals, the M/R ratios, and heating temperatures.

Keywords: Chemical synthesis; X-ray diffraction; Light absorption and reflection

1. Introduction

Phosphates are transformed to other phosphates in hydrolysis and dehydration reactions at elevated temperatures [1–7]. There are polyphosphate, *cyclo*-phosphate, and ultraphosphate in a group of condensed phosphates. Polyphosphate has a chain structure in which PO_4 unit shares two oxygen atoms, *cyclo*-phosphate has a cyclic structure and ultraphosphate has a network structure [8]. Phosphates have been used for ceramic materials, catalysts, fluorescent materials, pigments, etc. [9].

The addition of rare earth elements gives higher functional properties to the material [10]. In previous work, formation of binary *cyclo*-tetraphosphate was studied by replacing copper or magnesium with rare earth elements in synthesis of *cyclo*-tetraphosphates [11]. Further, surface properties of the mixed phosphates were investigated to clarify the role of rare earth elements. It was observed in copper salt that thermal product changed from *cyclo*-tetraphosphate to pyrophosphate by the addition of rare earth element. This change of thermal products depended on the kind of added rare earth element. In magnesium salt, the change of thermal products was not observed, magnesium *cyclo*-tetraphosphate was formed, in spite of the addition of rare earth element. Magnesium *cyclo*-tetraphosphate has increased the amounts of acidic sites by the addition of rare earth elements. The addition of rare earth elements had influence on formation and properties of condensed phosphates.

Transition metal orthophosphate has been used as an inorganic pigment. This material has good heat and light resistance for deterioration. However, there is a weak point, which is a certain degree of solubility for acidic and basic solution.

---

[*] Corresponding author. Fax: +81 75 753 5447.
E-mail address: h.onoda@materials.mbox.media.kyoto-u.ac.jp (H. Onoda).

doi:10.1016/j.jallcom.2004.12.076

On the other hand, rare earth phosphates are insoluble for acidic and basic solution. Consequently, the addition of rare earth cation had the anticipation to improve the acid and base resistance of inorganic phosphate pigments. Furthermore, because particle shape and size distribution have been interested on many viewpoints, their colors, acid and base resistance, and so on, the study about the particle shape and size distribution is important for development of new inorganic functional materials.

In this work, the influence of addition of Y, La, Ce, and Nd on formation and properties, that is, particle shape and size distribution, specific surface area, hue, acid and base resistance of Cu, Mn, and Co pyrophosphates were investigated from the view points of the kind of transition metals, rare earth elements, the ratio of transition metal/rare earth element, and heating temperature.

2. Experimental

Some rare earth oxides (Y_2O_3, La_2O_3, CeO_2, and Nd_2O_3) were mixed with basic copper carbonate in the mole ratio of Cu/R = 10/0, 9/1, and 8/2 (R: Y, or La, Ce, Nd). Manganese and cobalt carbonate were the same manner with copper carbonate. Ammonium dihydrogenphosphate was added to these mixtures in the mole ratio of P/(2M + 3R) = 1/2 (M: Cu, or Mn, Co). These ratios are the same with those of pyrophosphates, $M_2P_2O_7$, $M_{1.8}R_{0.2}(P_2O_7)_{1.05}$, and $M_{1.6}R_{0.4}(P_2O_7)_{1.1}$. Then thermal behavior of these mixtures was analyzed by differential thermal analyses (DTA), X-ray diffraction (XRD), and Fourier transform infrared spectroscopy (FT-IR). DTA curves were measured with a Shimadzu DTA50 at a heating rate of 10 °C/min under air condition. X-ray diffraction patterns were recorded on a Rigaku Denki RINT2000M X-ray diffractometer using monochromated Cu Kα radiation. The IR spectra were recorded on a Shimadzu FT-IR spectrometer FT-IR8600 with a KBr disk method.

The thermal products were characterized by scanning electron micrographs (SEM), particle size distribution, specific surface area, ultraviolet–visible (UV–vis) reflectance spectra, and fluorescence spectra. SEM images were observed using Hitachi F-4300. Particle size distribution was measured with laser diffraction/scattering particle size distribution HORIBA LA-910. Specific surface areas of phosphates were calculated from the amount of nitrogen gas adsorbed at the temperature of liquid nitrogen by BET method with Belsorp mini from BEL Japan Inc. UV–vis reflectance spectra were measured with a Shimadzu UV-3101PC. Fluorescence spectra were measured with a Hitachi F4500.

Furthermore, the acid and base resistance was estimated in following method. The 0.1 g of thermal products were allowed to stand in 100 ml of 0.1 wt% sulfuric acid or 0.1 wt% sodium hydroxide solution for 1 day. Then, solid was removed off by filtration, the solution was diluted with nitric acid. The concentrations of phosphorus, cobalt, and rare earth cation were measured by inductively coupled plasma (ICP). As a resistance estimation, the solubility (%) was calculated for the concentration which thermal products were completely dissolved. The ICP estimation was measured with Shimadzu ICPS-8000.

3. Results and discussion

3.1. Thermal behavior of the mixtures

Fig. 1 shows DTA curves of samples in various ratios. All samples had an endothermic peak at 200 °C due to volatilization of ammonia. By the addition of neodymium, some exothermic peaks appeared between 250 and 380 °C in DTA curves of copper samples (Fig. 1(a and b)). The manganese sample had large exothermic peak at 335 °C (Fig. 1(c)). This peak was considered to be due to formation of $MnHPO_4$ from XRD and IR analyses [12,13]. The broad endothermic peak at 500 °C was considered to be due to dehydration condensation of $MnHPO_4$ to $Mn_2P_2O_7$. By the addition of neodymium, small exothermic peaks at 270 and 410 °C were observed in DTA curve of sample in Mn/Nd = 8/2 (Fig. 1(d)). These peaks were thought to be related with manganese and neodymium phosphates, respectively. The cobalt sample had less endothermic and exothermic peak (Fig. 1(e)). Sample in Co/Nd = 8/2 had similar peaks on DTA curve with sample in Mn/Nd = 8/2 (Fig. 1(d and f)). The addition of rare earth elements gave new exothermic peaks in DTA curves of copper, manganese, and cobalt phosphates.

Samples heated at lower temperature had lower crystalline phase. Fig. 2 shows XRD patterns of samples

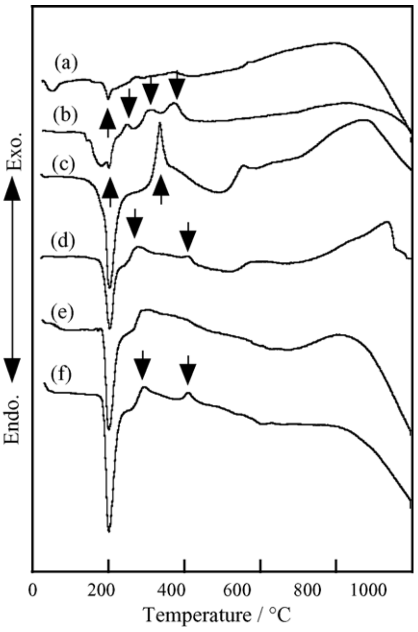

Fig. 1. DTA curves of samples: (a) Cu, (b) Cu/Nd = 8/2, (c) Mn, (d) Mn/Nd = 8/2, (e) Co, and (f) Co/Nd = 8/2.

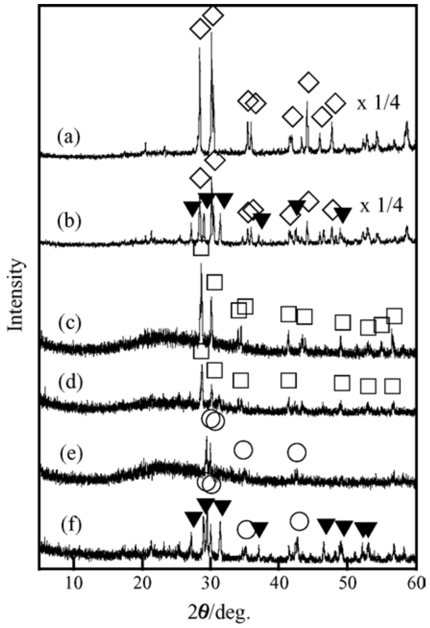

Fig. 2. XRD patterns of samples prepared in various systems heated at 1000 °C: (a) Cu, (b) Cu/Nd = 8/2, (c) Mn, (d) Mn/Nd = 8/2, (e) Co, and (f) Co/Nd = 8/2; (◇) $Cu_2P_2O_7$, (▼) $NdPO_4$, (□) $Mn_2P_2O_7$, and (○) $Co_2P_2O_7$.

heated at 1000 °C. The copper samples had strong XRD peaks than manganese and cobalt samples. Copper, manganese, and cobalt pyrophosphate were formed in each sample (Fig. 2(a, c, and e)). By the addition of neodymium, neodymium orthophosphate was formed with each pyrophosphate (Fig. 2(b, d, and f)). Lanthanum orthophosphate was crystallized at lower temperature than other rare earth phosphates. The addition of rare earth cation had little influence on IR spectra of transition metal pyrophosphate.

Target transition metal pyrophosphates were formed at high temperature in these systems. By the addition of rare earth cation, rare earth orthophosphates were formed with each transition metal pyrophosphate.

3.2. Powder properties of thermal products

Particle shape and size distribution have been interested on many viewpoints, their colors, acid and basic resistance, and so on. Therefore, the study about the particle shape and size distribution is important for development of new inorganic functional materials. From SEM images, all samples in this work did not have specified shape. The addition of rare earth element had less influence on particle shape of samples.

Fig. 3 shows particle size distribution of thermal products at 700 °C. The large part of phosphate powder had the size distribution from 200 to 1 μm. The particle size distribution of manganese samples consisted of two normal distributions. By the addition of rare earth cation, particle size became a little larger. Samples heated at 1000 °C had same tendency on particle size distribution with samples heated at 700 °C.

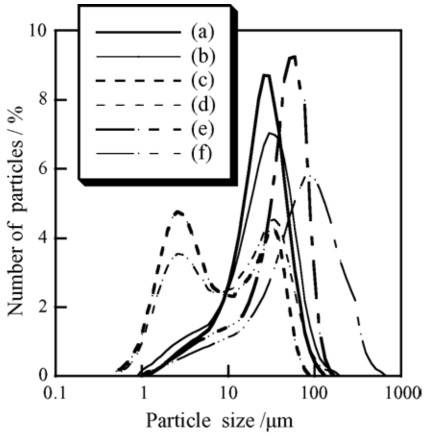

Fig. 3. Particle size distribution of thermal products at 700 °C: (a) Cu, (b) Cu/Nd = 8/2, (c) Mn, (d) Mn/Nd = 8/2, (e) Co, and (f) Co/Nd = 8/2.

Table 1 shows specific surface area of thermal products at 700 °C. The addition of rare earth cation made specific surface area small. If sample had been the mixture of transition metal pyrophosphate and neodymium orthophosphates, specific surface area of samples in M/R = 8/2 was the total amount of 0.8-fold area of transition metal pyrophosphates and 0.2-fold area of rare earth orthophosphates. The sample in this work had enough lower specific surface area than the mixture. Therefore, it was considered that transition metal–rare earth phosphate composite particles were formed in these conditions.

3.3. Hue of thermal products

Fig. 4 shows UV–vis reflectance spectra of thermal products at 1000 °C. The color of copper, manganese, and cobalt samples was sky blue, white, and purple, respectively. By the addition of neodymium, UV–vis reflectance spectra had new peaks at 356, 430, 470, 513, 525, 583, 682, 750, and 804 nm. These peaks were assigned to the $^4I_{9/2} \rightarrow {}^4D_{3/2}$, $^4I_{9/2} \rightarrow {}^2P_{1/2}$, $^4I_{9/2} \rightarrow {}^2G_{9/2} + {}^2D_{3/2}$, $^4I_{9/2} \rightarrow {}^4G_{9/2}$, $^4I_{9/2} \rightarrow {}^4G_{7/2}$, $^4I_{9/2} \rightarrow {}^4G_{5/2} + {}^2G_{9/2}$, $^4I_{9/2} \rightarrow {}^4F_{9/2}$, $^4I_{9/2} \rightarrow {}^4S_{3/2} + {}^4F_{7/2}$, and $^4I_{9/2} \rightarrow {}^2H_{9/2} + {}^4F_{5/2}$ transition of Nd^{3+} ions, respectively [14]. The addition of neodymium had little influence on hue of transition metal pyrophosphates. The addition of yttrium, lanthanum, and cerium had little influence on UV–vis reflectance spectra. Furthermore, the transition metal pyrophosphates had little fluorescence by the addition of yttrium, lanthanum, cerium, and neodymium.

Table 1
Specific surface area of thermal products at 700 °C

M	Specific surface area (m^2g^{-1})		
	M/Nd = 10/0	M/Nd = 9/1	M/Nd = 8/2
Cu	4.2	2.7	2.0
Mn	7.9	6.6	4.5
Co	2.9	1.7	1.7

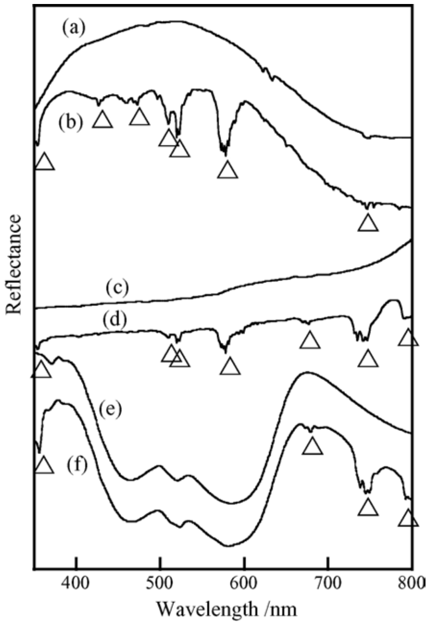

Fig. 4. UV–vis reflectance spectra of thermal products at 1000 °C: (a) Cu, (b) Cu/Nd = 8/2, (c) Mn, (d) Mn/Nd = 8/2, (e) Co, and (f) Co/Nd=8/2; (△) Nd^{3+}.

3.4. Acid and base resistance estimation

Fig. 5 shows acid resistance of cobalt pyrophosphates. By the addition of neodymium, the solubility of thermal products became lower. Acid resistance also improved with heating temperature. Rare earth phosphates were much insoluble than transition metal pyrophosphates. The formation of transition metal pyrophosphate–rare earth orthophosphate composite particles was considered to cause higher acid resistance.

Fig. 6 shows base resistance of cobalt pyrophosphate. The solubility in basic solution was lower than that in acidic solution. The elution of cobalt and neodymium was not confirmed because of formation of their hydroxide. Cobalt and neodymium hydroxides were considered to make the contact area of the phosphates with basic solution decrease. Base resistance of thermal products improved by the addition of neodymium. The solubility in basic solution became lower with the increase of heating temperature.

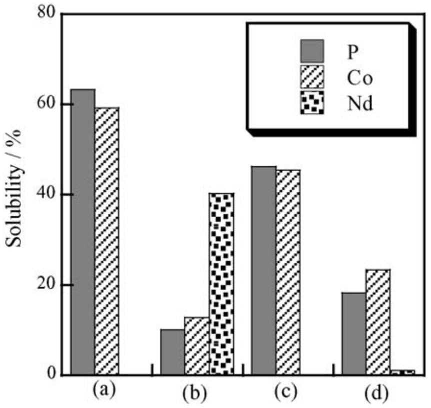

Fig. 5. Acid resistance of thermal products prepared in various conditions: (a) Co, 700 °C, (b) Co/Nd = 8/2, 700 °C, (c) Co, 1000 °C, and (d) Co/Nd = 8/2, 1000 °C.

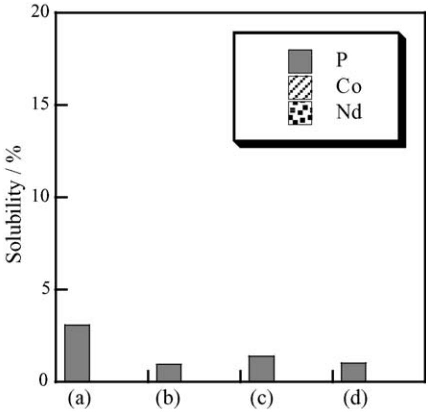

Fig. 6. Base resistance of thermal products prepared in various conditions: (a) Co, 700 °C, (b) Co/Nd = 8/2, 700 °C, (c) Co, 1000 °C, and (d) Co/Nd = 8/2, 1000 °C.

4. Conclusion

Rare earth orthophosphate was formed with transition metal pyrophosphate by the addition to formation systems of transition metal pyrophosphate. From specific surface area of thermal products, transition metal pyrophosphate–rare earth orthophosphate composite particles were considered to be formed. Thermal products did not have specified shape by the addition of rare earth cation, particle size became a little larger. The addition of rare earth cation had little influence on hue of transition metal pyrophosphates. Thermal product had little fluorescence by the addition of rare earth cation. The addition of rare earth cation improved the acid and base resistance of thermal products which is a weak point for use of inorganic pigment.

References

[1] M. Tsuhako, S. Ikeuchi, T. Matsuo, I. Motooka, M. Kobayashi, Bull. Chem. Soc. Jpn. 52 (1979) 1034.
[2] H. Onoda, H. Nariai, H. Maki, I. Motooka, Mater. Chem. Phys. 73 (1) (2002) 19.
[3] H. Onoda, H. Nariai, H. Maki, I. Motooka, J. Mater. Synth. Process. 10 (3) (2002) 121.
[4] M.T. Averbuch-Pouchat, A. Durif, Topics in Phosphate Chemistry, World Scientific Publishing Co. Pte. Ltd., Singapore, 1996.
[5] H. Onoda, A. Takenaka, K. Kojima, H. Nariai, Mater. Chem. Phys. 82 (1) (2003) 194.
[6] H. Onoda, H. Nariai, H. Maki, I. Motooka, Mater. Chem. Phys. 78 (2) (2002) 400.
[7] H. Onoda, H. Nariai, H. Maki, I. Motooka, Phosphorus Res. Bull. 9 (1999) 69.
[8] H.Y.-P. Hong, Acta Cryst. B30 (1974) 468.

[9] H. Onoda, H. Nariai, A. Moriwaki, H. Maki, I. Motooka, J. Mater. Chem. 12 (6) (2002) 1754.
[10] N.E. Topp, in: J. Shiokawa, G. Adachi (Eds.), Chemistry of the Rare Earth Elements, Kagakudojin, Kyoto, 1974, p. 184.
[11] H. Onoda, H. Nariai, H. Maki, I. Motooka, Phosphorus Res. Bull. 12 (2001) 139.
[12] D.E.C. Corbridge, E.J. Lowe, J. Chem. Soc. 493 (1954) 4555.
[13] H. Onoda, N. Sugino, K. Kojima, H. Nariai, Mater. Chem. Phys. 82 (3) (2003) 831.
[14] M. Yamazaki, Y. Yamamoto, S. Nagahama, N. Sawanobori, M. Mizuguchi, H. Hosono, J. Non-Cryst. Solids 241 (1998) 71.